Intermediate valence metals: Current issues

Jon Lawrence

University of California, Irvine

http://www.physics.uci.edu/~jmlawren/Research.html

The ground state of rare earth intermediate valence (IV) metals is that of a heavy mass Fermi liquid. The transport, optical conductivity and dHvA signals reflect the existence of a Fermi surface with strongly renormalized masses. On the other hand, properties such as the susceptibility, specific heat, valence and spin dynamics that are dominated by the spin fluctuations, which are highly localized, can be understood qualitatively (and sometimes quantitatively) as those of a collection of non-interacting Anderson/Kondo impurities. We will show that anomalies exist in some compounds both in the low temperature behavior and in the rate of crossover from Fermi liquid to local moment behavior.

Collaborators

Los Alamos (LANL):	Joe Thompson, John Sarrao, Mike Hundley , Eric Bauer	
	Crystal growth, $\chi(T)$, C(T), R_H, $\rho(H)$	
NHMFL/LANL	Alex Lacerda, Myung-Hwa Jung, Neil Harrison	
	$\rho(H)$, M(H), dHvA	
LBL `	Corwin Booth	$n_f(T)$ (L_3 XRA)
Shizuoka U.	Takao Ebihara	Crystal growth; dHvA
U. Nevada, Las Vegas	Andrew Cornelius	M(H); dHvA
Temple U.	Peter Riseborough	Theory (NCA)
IPNS @ ANL	Ray Osborn	$\chi''(\omega)$ (neutron scattering)
HFBR @ BNL	Steve Shapiro	••• ••• •••

Intermediate Valence Compounds

$CeSn_3$	Fermi liquid (FL)	$YbAgCu_4$, $YbTlCu_4$
$CePd_3$	FL with anomalies	$YbMgCu_4$, $YbAl_3$
$Ce_3Bi_4Pt_3$	Kondo Insulators	YbB_{12}
α-Ce/γ-Ce	Valence Transitions	$YbInCu_4$

***Archetypal class of solids subject to electron correlations*.**
More complex than TM's (e.g. Pd) or 3D one-band Hubbard Model
Less complex than TM oxides (e.g. high-T_c) which have
multiple bands, 2D character, possible hidden order, QCP

Comparison to Heavy Fermions (HF)

HF	***IV***
Low symmetry (tet, hex)	High symmetry (cubic)
Anisotropy (sometimes 2D effects)	Isotropic (3D)
CF doublet ground state:	CF unimportant:
$T_K < T_{cf}$	$T_K > T_{cf}$
$N_J = 2J + 1 = 2$	$N_J = 6$ (Ce); 8 (Yb)
Proximity to QCP:	Proximity to Kondo Insulator:
AF correlations	Hybridization gap; No AF correlations

GROUND STATES:

Very heavy FL	Moderately heavy FL
Marginal FL	Kondo insulator
HF superconductivity	
Miniscule moment AF	(And: first order valence transitions)

In this talk we focus on IV metals, with FL ground states

High temperature limit:

LOCAL MOMENT PARAMAGNET

Integral valence: $n_f \to 1$ $z = 2+n_f = 3$ Yb $4f^{13}(5d6s)^3$

$z = 4-n_f = 3$ Ce $4f^{1}(5d6s)^3$

Curie Law: $\chi \to C_J/T$ $T\chi/C_J \to 1$

$C_J = N\, g^2\, \mu_B^2\, J(J+1)/\, 3\, k_B$ $J = 7/2$ (Yb)

$5/2$ (Ce)

Full moment entropy: $S \to R\, ln(2J+1)$

$\Downarrow$

CROSSOVER

at Characteristic temperature T_0

$\Downarrow$

Low temperature limit:

FERMI LIQUID

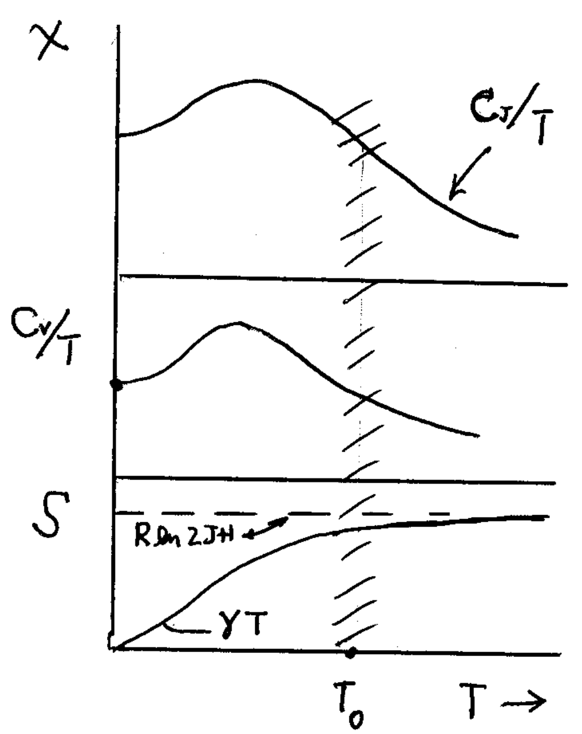

Nonintegral valence ($n_f < 1$)

Yb $4f^{14-nf}(5d6s)^{2+nf}$

Ce $4f^{\,nf}(5d6s)^{4-nf}$

Pauli paramagnet:

$\chi(0) \sim \mu_B^2\, N(\varepsilon_F)$

Linear specific heat:

$S \sim C_v \sim \gamma\, T$

$\gamma = (1/3)\, \pi^2\, N(\varepsilon_F)\, k_B^2$

Example: $YbAl_3$ ground state

Ground state Valence (IV):

$YbAl_3$ $(5d6s)^{2.75}\,4f^{13.25}$ $n_f = 0.75$ IV

Pauli paramagnetism:

$YbAl_3$: $\chi(0) = 0.005$emu/mol

Specific heat:

In a Fermi liquid, $\gamma = \{\pi^2 k_B^2\ N_A\ Z / (3\ h^3 \pi^2\ N/V)^{2/3}\}\ m^*$

For simple metals (e.g. K): $\gamma = 2$mJ/mol-K^2 and $m^* = 1.25m_e$

For $YbAl_3$: $\gamma_m = 40$mJ/mol-K^2 and $m^* = 20m_e$

$\rightarrow$ "Moderately HEAVY FERMION" compound

C/T vs. T^2 for $YbAl_3$

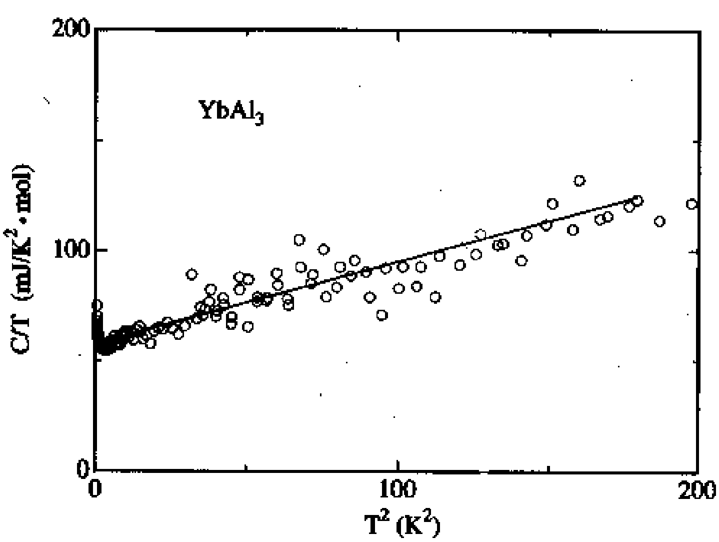

Ebihara et al
Physica B281&282
(2000) 754

Spin fluctuation spectra $YbInCu_4$

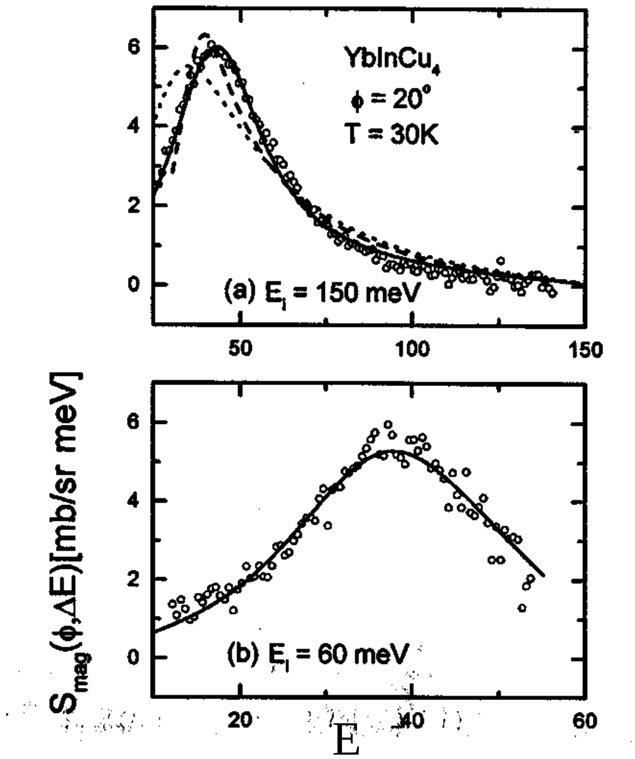

$YbInCu_4$
Magnetic scattering S_{mag} vs. E at two incident energies E_i

Lawrence, Osborn et al
PRB59 (1999) 1134

Lorentzian power spectrum

$$\chi''(Q,E) = (n(E)+1)\, f^2(Q)\, \chi'(Q)\, E\;\; P(E)$$

$$P(E) = (\Gamma/2)\, \{(E - E_0)^2 + \Gamma^2)^{-1} + (E + E_0)^2 + \Gamma^2)^{-1} \}$$

$f^2(Q)$: 4f form factor

Q-dependence: In one of the only single x-tal IV metals studied ($YbInCu_4$) (Lawrence, Shapiro et al, PRB55 (1997) 14467) the scattering at five **Q** in the BZ showed ***no dependence of Γ or E_0 on Q*** and only a weak (15%) dependence of χ' on **Q**.

Q-independent, broad Lorentzian response $\Rightarrow$

Primary excitation is a local, highly damped spin fluctuation (oscillation) at characteristic energy $E_0 = k_BT_0$

WHERE IS THE FERMI LIQUID SCATTERING?

Anderson Impurity Model (AIM)

$$
\begin{aligned}
H_{AI} &= H_0 + H(i) + V(i) \\
H_0 &= \sum_k \varepsilon_k \mathbf{n}_k \\
H_f(i) &= E_f\,\mathbf{n}(i) + U\,\mathbf{n}_{f\uparrow}(i)\,\mathbf{n}_{f\downarrow}(i) \\
V(i) &= \sum_k V_{kf}\,\mathbf{c}_k^+\,\mathbf{f}(i) + c.c.
\end{aligned}
$$

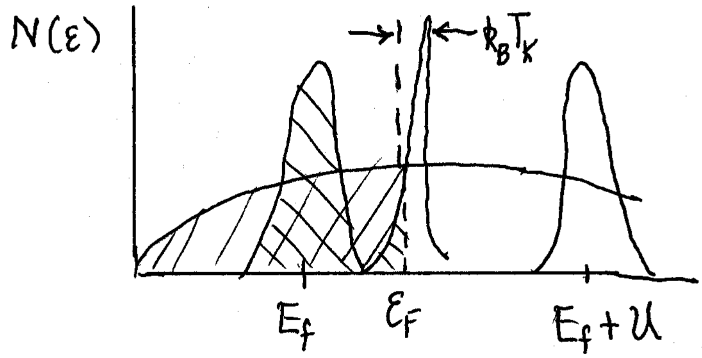

Although intended for dilute alloys, (e.g. $La_{1-x}Ce_x$) because the spin fluctuations are local, the AIM describes much of the physics of periodic IV compounds.

Characteristic features:

Kondo Resonance:

a low energy peak in the renormalized density-of-states (DOS) at

$$k_BT_K \sim \varepsilon_F \exp\{-E_f/(N_J V^2 N(\varepsilon_F))\}$$

Spin/valence fluctuation:* *localized, damped oscillator with ***characteristic energy*** k_BT_K: $\chi'' \sim \chi(T)\,E\,\Gamma/((E-E_0)^2 + \Gamma^2)$ $E_0 = k_BT_K$

Crossover:

from ***Low temperature local Fermi liquid***

(nonintegral valence, Pauli paramagnetism, linear specific heat)

to ***local moment*** behavior for $T > T_K$

(integral valence, Curie law magnetism, R*ln*(2J+1) entropy)

Universality: Properties scale as T/T_K, E/k_BT_K, μ_BH/k_BT_K

Wilson ratio: $(\pi^2 R/3C_J)\chi(0)/\gamma \cong 1 + (1/2J)$

VERY MUCH LIKE ACTUAL BEHAVIOR OF IV COMPOUNDS

$YbAl_3$: Susceptibilty, Specific Heat, 4f occupation Data vs. AIM

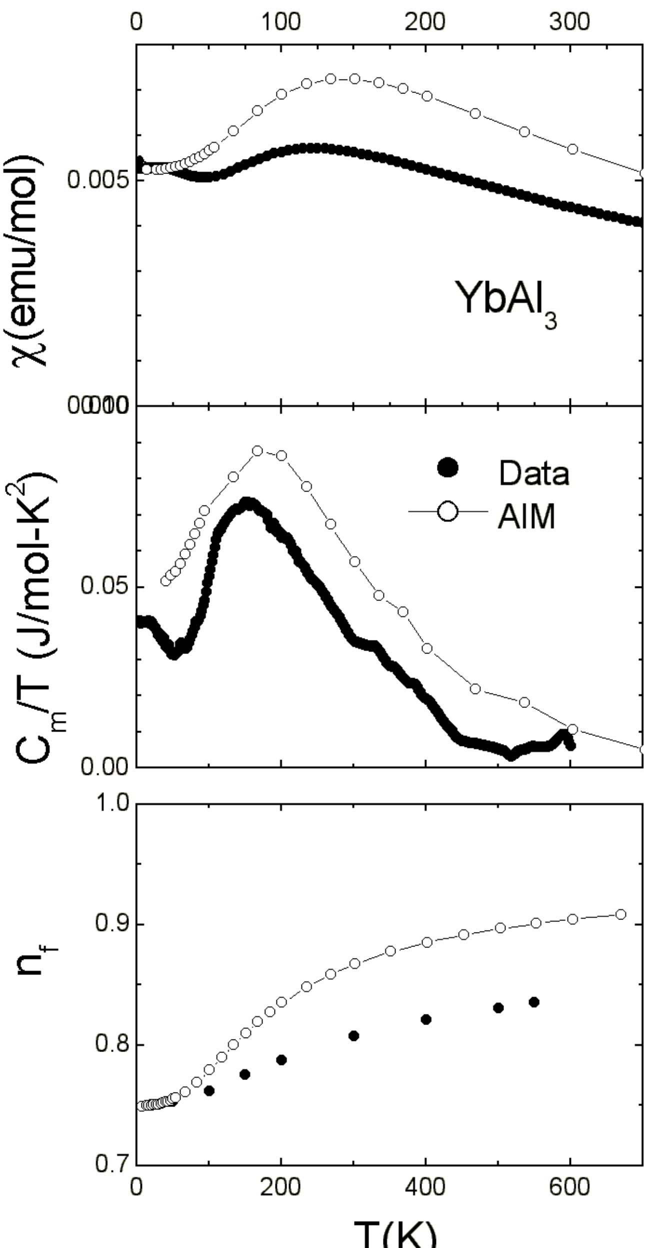

Cornelius et al
PRL88 (2002) 117201

AIM parameters

(Chosen to fit $\chi(0)$, $n_f(0)$ and $\gamma(LuAl_3)$)

W = 4.33eV
E_f = -0.58264eV
V = 0.3425eV
T_K = 670K

Wilson ratio:
The AIM predicts that the normalized ratio of susceptibility to specific heat should be

$(\pi^2 R/3C_J)\chi(0)/\gamma \cong 1 + (1/2J) = 8/7$

The experiment gives 1.3-1.4.

Fits to the AIM: $n_f(T)$

O data
___ AIM

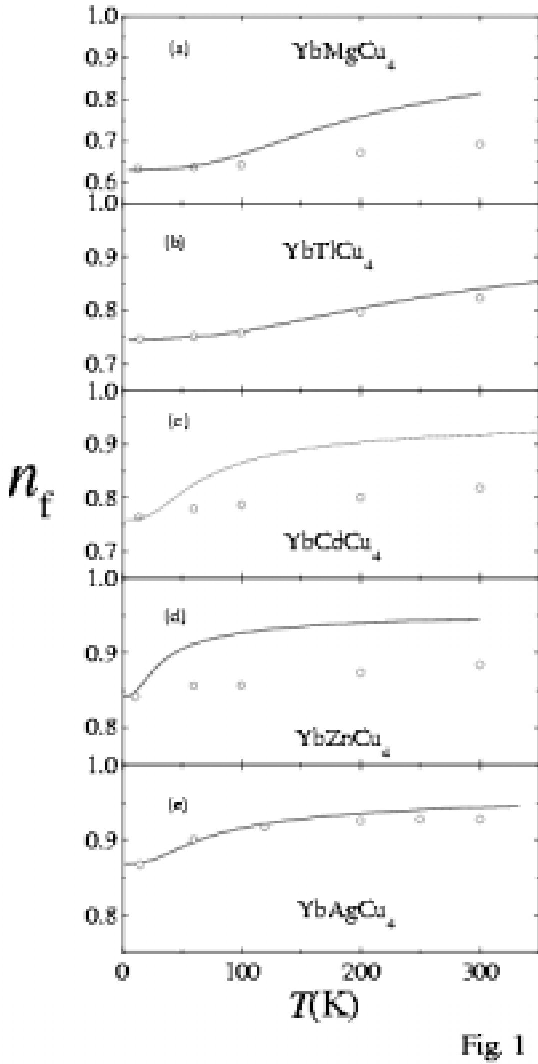

Fig. 1 Lawrence et al
PRB 63 (2001) 054427

Note: Good quantitative fits for $YbAgCu_4$ and $YbTlCu_4$.
but **Slow crossover** for $YbMgCu_4$, $YbCdCu_4$ and $YbZnCu_4$

Fits to the AIM: $\chi(T)$

Symbols: data
Lines: AIM

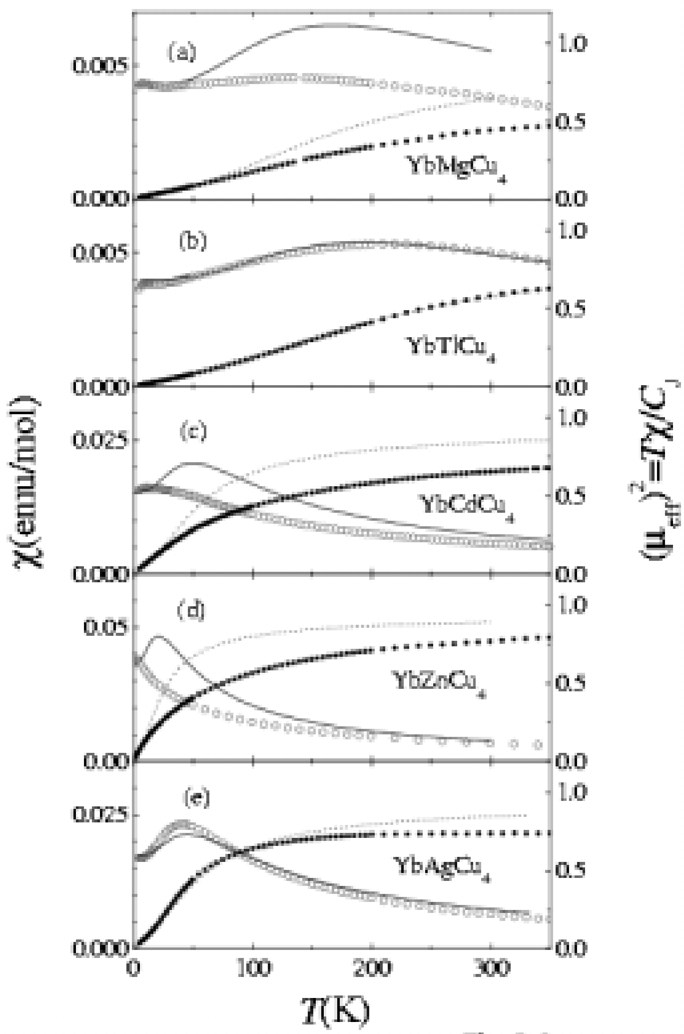

Fig. 2 Lawrence et al

PRB 63 (2001) 054427

Note: Good quantitative fits for $YbAgCu_4$ and $YbTlCu_4$
but **Slow crossover** for $YbMgCu_4$, $YbCdCu_4$ and $YbZnCu_4$

Low temperature spin dynamics

At low temperature the neutron scattering exhibits an inelastic (IE) q-independent Kondo peak:

$\chi''(E) = \Gamma E / ((E- E_0)^2 + \Gamma^2)$
+ anti-Stokes

representing the strongly damped local excitation. For $YbAl_3$ the parameters of the low temperature peak are E_0 = 40meV and Γ = 25meV which compare favorably to the AIM values E_0 = 40meV and Γ = 25meV

Murani, PRB 50 (1994) 9882

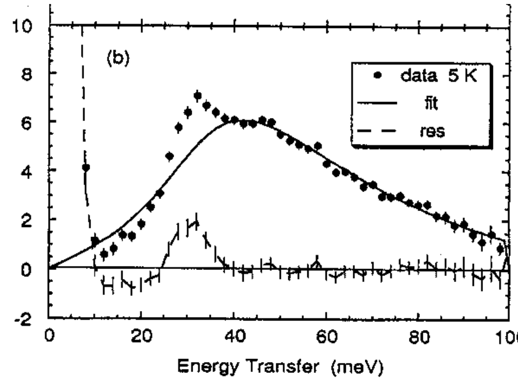

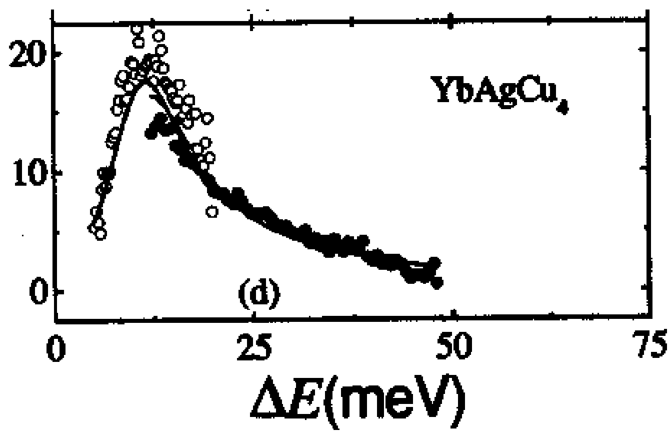

For $YbAgCu_4$ the parameters of the AIM fit E_0 = 11meV and Γ = 7meV are equal to the measured values

Overall agreement with AIM (NCA):

Two parameters (E_f, V) chosen to fit $\chi(0)$ and $n_f(0)$

$YbAgCu_4$: Fits T dependence of χ and n_f
and low T neutron spectral parameters

$YbTlCu_4$: Fits T dependence of χ and n_f

$YbAl_3$: Fits neutron spectral parameters at T = 0
Fits specific heat coefficient to 20%
Fits T_{max} for χ and γ=C/T to 20%

BUT: AIM predictions evolve more rapidly with temperature than the data for $YbMgCu_4$, $YbCdCu_4$ and $YbAl_3$ and there are low-T anomalies in the latter compound.

TRANSPORT BEHAVIOR OF IV COMPOUNDS

The AIM predicts a finite resistivity at T = 0) (unitary scattering from the 4f impurity.

In an IV compound, where the 4f atoms form a periodic array, the resistivity must vanish.

(Bloch’s law)

Typically in IV compounds

$\rho \sim A\,(T/T_0)^2$

This is a sign of **Fermi Liquid “coherence”** among the spin fluctuations.

In $YbAl_3$ this occurs below the “**coherence temperature**”

$T_{coh} \sim 40K$

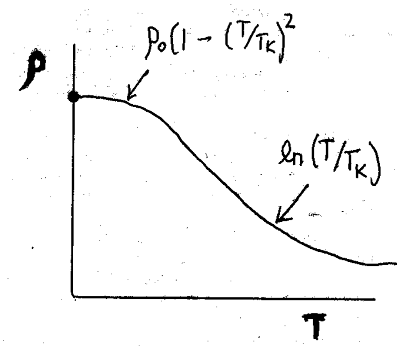

$YbAl_3$ ρ vs T^2

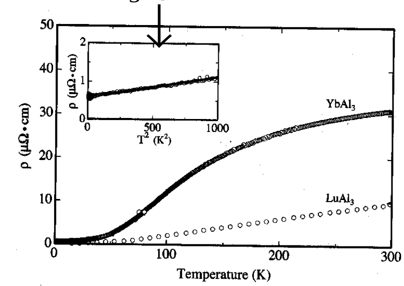

Fig. 1. Temperature dependence of the electrical resistivity of $YbAl_3$ and $LuAl_3$. The inset shows the T^2-dependence of the resistivity.

Ebihara et al
Physica B281&282 (2000) 754

Two theoretical approaches to the Fermi Liquid

Band theory: Itinerant 4f electrons (LDA) with correlations:

a) LDA + U, or
b) Add Kondo physics through Renormalized Band Method

Anderson Lattice Model: Localized 4f electrons

a) Ignore intersite contributions

Yoshimori and Kasai, Journ. Mag. Mag. Mat. 31-34 (1983) 475

b) Large $N_J = 2J+1$ methods

Georges et al, PRL 85 (2000) 1048
Ono and Kuroda, Journ. Phys. Soc. Japan 60 (1991) 3475

c) Dynamic Mean Field

Jarrell et al, PRB 55 (1997) R3332

De Haas van Alphen and the Fermi surface

Figures from Ebihara et al, J Phys Soc Japan 69 (2000) 895

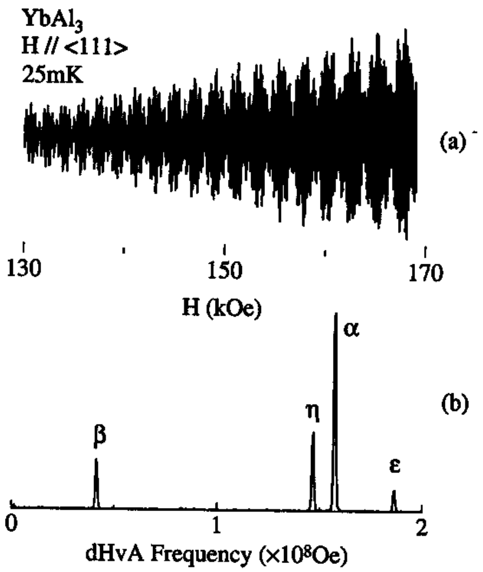

ig. 1. (a) DHvA oscillation and (b) its FFT spectrum for the apan field along ⟨111⟩ in $YbAl_3$.

The **de Haas van Alphen** experiment measures oscillations in the magnetization as a function of inverse magnetic field.

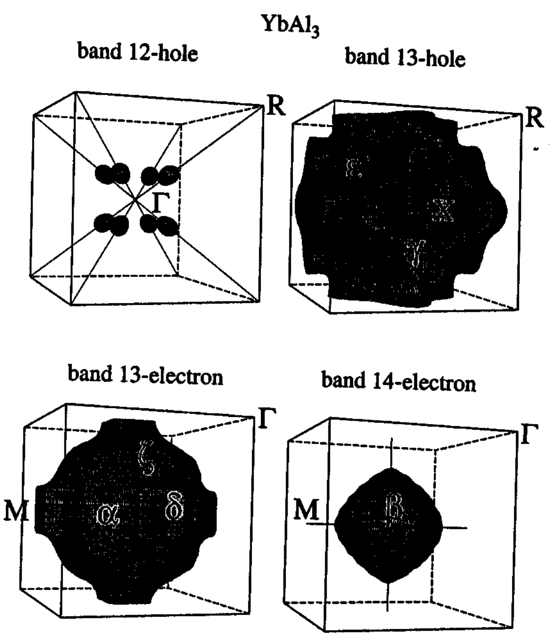

Fig. 7. Modified Fermi surfaces in $YbAl_3$. The band 13-hole and the band 13-electron Fermi surface represent the same Fermi surface.

The frequency of the oscillations is determined by the areas S of the extremal cross sections of the Fermi surface in the direction perpendicular to the applied field.

$$M = A \cos(2\pi F/H)$$

$$F = (hc/2 \pi e)\, S$$

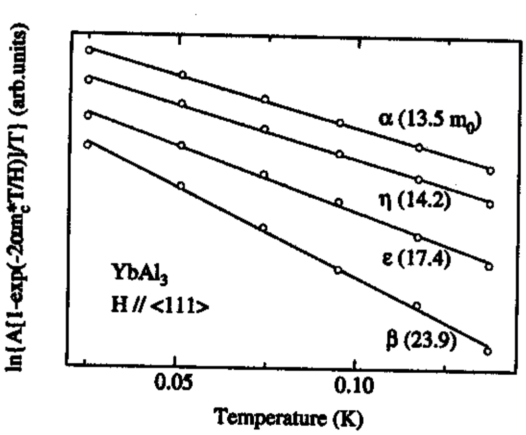

Fig. 3. Mass plot for the field along ⟨111⟩ in $YbAl_3$.

The temperature dependence of the amplitude determines the effective mass m*

$$A = 1/\sinh(Qm^*T/H)$$

where Q is a constant

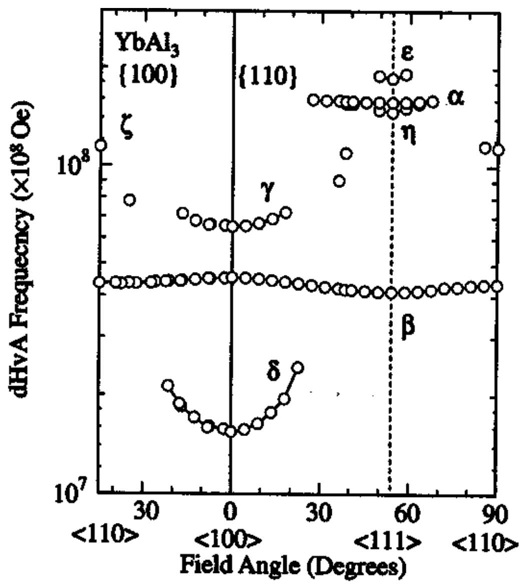

Fig. 2. Angular dependence of the dHvA frequency in $YbAl_3$.

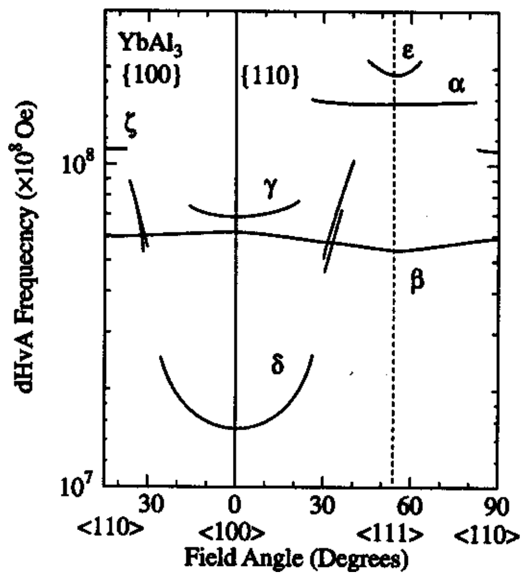

EXPT

THEORY

For IV compounds LDA gives the correct extremal areas!

One-electron band theory (LDA) treats 4f electrons as itinerant.
It correctly predicts the topology of the Fermi surface as observed by dHvA.

But: **LDA strongly underestimates the effective masses!**

LDA badly overestimates the 4f band widths and consequently strongly underestimates the effective masses:

LDA: $m^* \sim m_e$

dHvA: $m^* \sim 15\text{-}25 m_e$

LDA also tends to make Yb compounds (including $YbAl_3$!!) be divalent.
Large masses and intermediate valence can be obtained by LDA + U

(For $YbAl_3$ the correct valence was obtained by forcing the 4f level energy in the LDA)

ANDERSON LATTICE

For a periodic IV compound the appropriate model is

$$H = \Sigma_k \varepsilon_k \mathbf{n}_k + \Sigma_i\{E_f\, \mathbf{n}_{fi} + U\, \mathbf{n}_{\mathbf{fi}\uparrow}\, \mathbf{n}_{\mathbf{fi}\downarrow} + \Sigma_k[V_{kf}\, \mathbf{c}^+_k \mathbf{f}_i + cc]\}$$

This leads to a coherent band structure with (renormalized) hybridized bands near the Fermi energy. The bands exhibit a hybridization gap; the Fermi level lies in the high DOS region due to the large admixture of 4f states. The large DOS is responsible for the large m*.

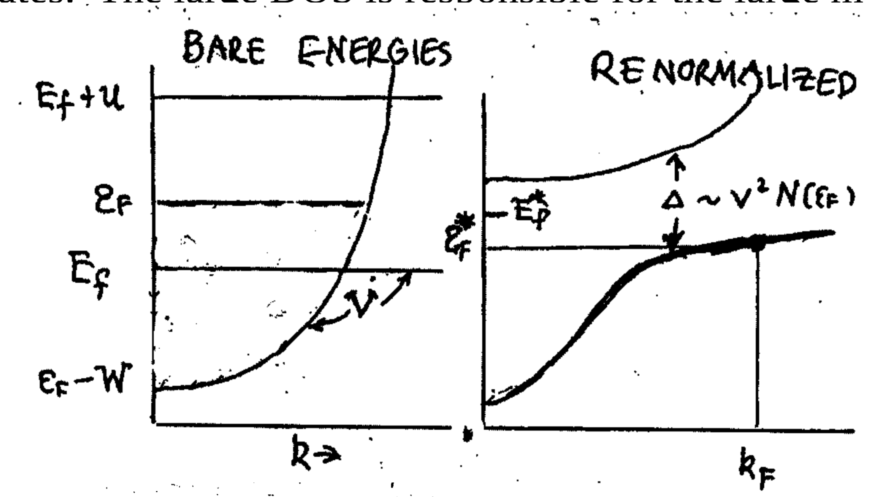

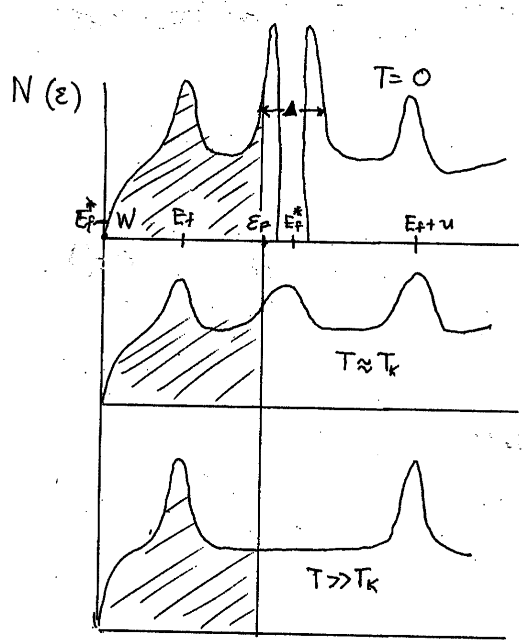

The structure renormalizes away with increasing temperature:

For very low $T << T_K$
Fully hybridized bands

For $T \sim T_{K,}$
No gap
Incoherent Kondo resonances

For $T >> T_K$
Local moments uncoupled from band electrons

Spin dynamics should exhibit:

Fermi liquid scattering across ε_F*

Q-dependent gap scattering, peaking at Zone Boundary

THESE HAVE NOT OBSERVED IN ANY IV METAL!!

Optical conductivity

BEST EVIDENCE FOR THE HYBRIDIZATION GAP AND ITS RENORMALIZATION WITH TEMPERATURE

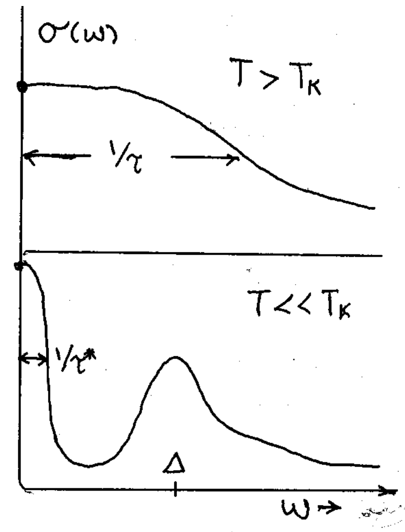

High temperature:

Normal Drude behavior:

$\sigma'(\omega) = (ne^2/m_b)\{\tau / (1 + \tau^2\omega^2)\}$

m_b is the bare band mass

τ is the relaxation time.

$\Downarrow$

CROSSOVER

$\Downarrow$

Low temperature:

1) IR absorption peak from transitions across hybridization gap
2) *Very* narrow Drude peak. Both m and τ renormalized.

$m_b \rightarrow \lambda\, m_b = m^*$ $\qquad \tau \rightarrow \lambda\, \tau = \tau^*$

$\sigma'(\omega) = ne^2\, [\tau^* / m^*]\, \{1 / (1 + \tau^{*2}\omega^2)\}$

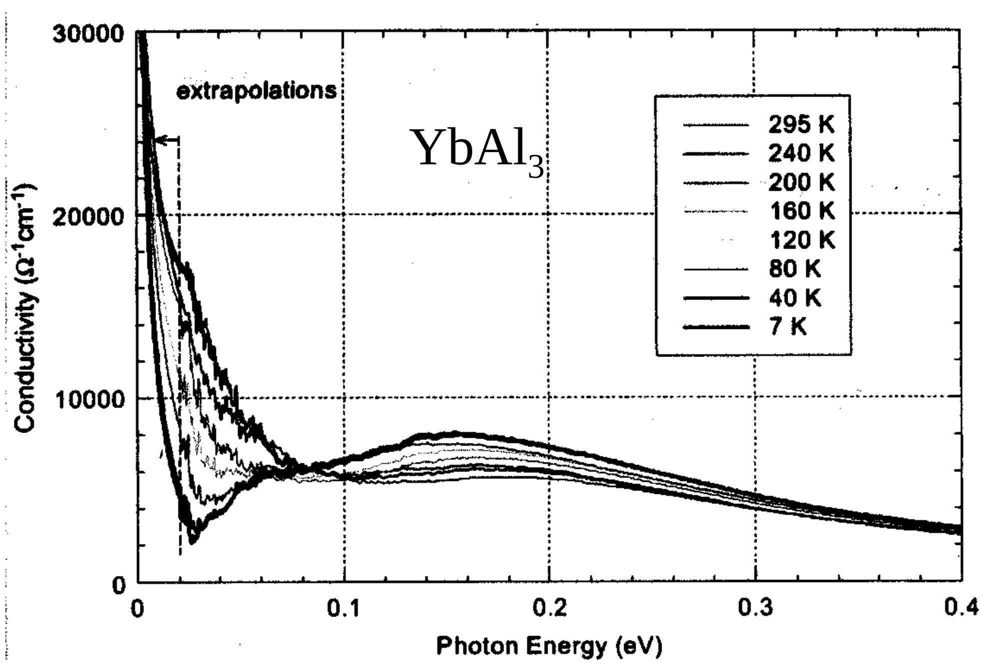

Okamura, Ebihara and Namba, cond-mat/0208006

RENORMALIZATION COMPLETE BELOW T_{coh} = 40K

Extended Drude analyses

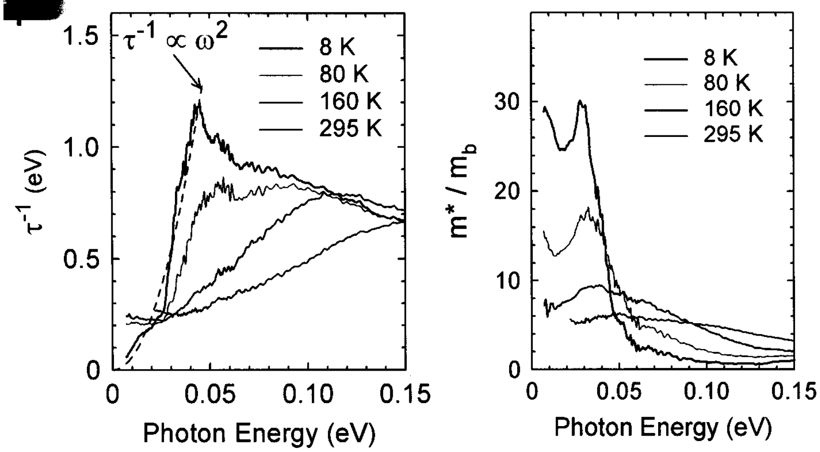

- Fermi liquid behavior ($1/\tau \sim \omega^2$)
- Mass enhancement (m^*/m_b =25-30)

→ Heavy-mass Fermi liquid

Assuming frequency-dependent scattering

$\sigma(\omega) = (ne^2/m_b)\,[\gamma(\omega) - i\,\omega]^{-1}$

then the mass enhancement

$m^* = \lambda m_b$

$\lambda(\omega) = -\mathrm{Im}[\gamma(\omega)]/\,\omega$

is both frequency and temperature dependent

For $YbAl_3$ this procedure gives m*~25-30, comparable to the dHvA masses.

$CePd_3$ optical conductivity

Development of renormalized Drude with decreasing temperature is connected with a transfer of spectral weight over large (eV) energy scales

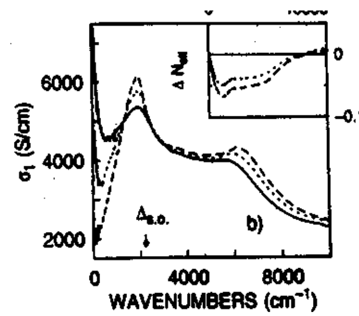

Beyermann et al, PRL 60 (1988) 216

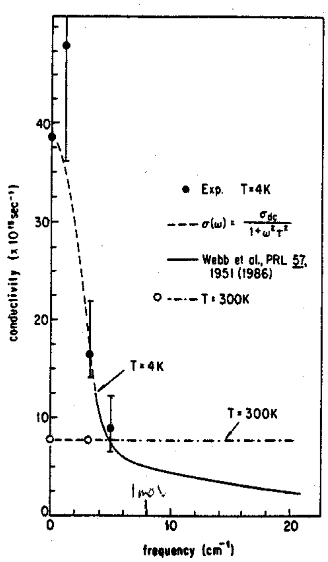

Bucher et al, PRB 53 (1996) R2948

Observation of the full renormalized Drude response requires microwave conductivity measurement
(using resonant cavity)

Webb et al, PRL 57 (1986) 1951

Assuming frequency-dependent scattering

$\sigma(\omega) = (ne^2/m_b)\,[\gamma(\omega) - i\,\omega]^{-1}$

then the mass enhancement

$m^* = \lambda m_b$

$\lambda(\omega) = -\mathrm{Im}[\gamma(\omega)]/\,\omega$

is both frequency and temperature dependent

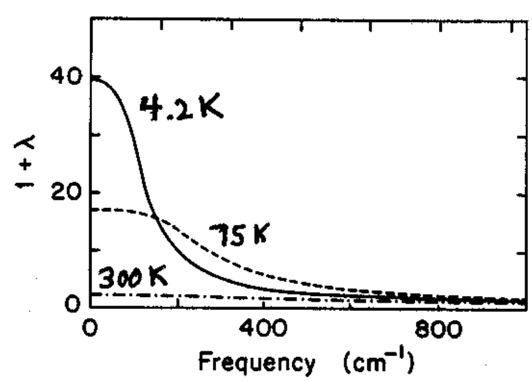

For $YbAl_3$ this procedure gives m*~25-30, comparable to the dHvA masses.

Two energy scales and slow crossover in the Anderson Lattice

While the transport behavior and the Fermi surface (dHvA) are affected by Fermi liquid coherence, we have seen that experimental quantities such as the specific heat, susceptibility, valence and spin dynamics are qualitatively in good accord with the predictions of the AIM over a broad range of temperature. This reflects highly localized spin/valence fluctuations

Nevertheless, recent theory for the Anderson Lattice suggests that the behavior of these latter quantities can differ in two ways from the predictions of the AIM:

1) Non-universal low temperature scale for coherence and/or Low temperature anomalies

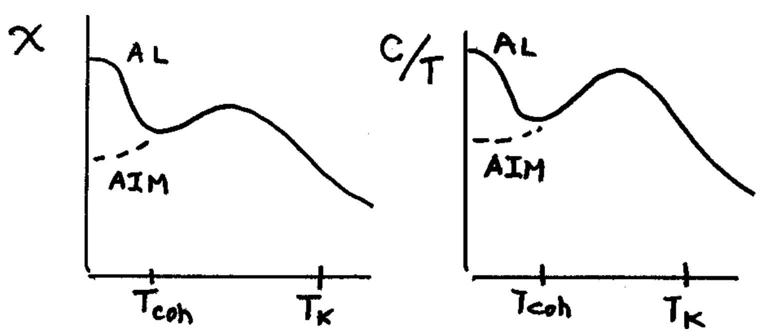

Antoine Georges et al, PRL 85 (2000) 1048
Ono and Kuroda, Journ. Phys. Soc. Japan 60 (1991) 3475

2) Slow crossover from Fermi Liquid to Local Moment

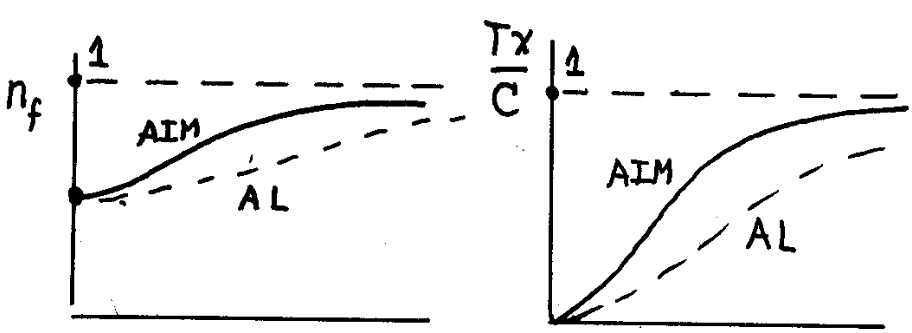

Mark Jarrell et al PRB55 (1997) R3332

Theory predicts that these differences become magnified when the conduction electron or hole density is low.

Slow crossover in $YbAl_3$

We have seen that slow crossover in $\chi(T)$ and $n_f(T)$ occurs for $YbXCu_4$
It has been correlated to electron density $n_e = 1/R_He$ determined from the Hall coefficient (Lawrence et al, PRB 63 (2001) 054427)

$YbAgCu_4$, $YbTlCu_4$ $n_e >$ 1e/atom No slow crossover

$YbMgCu_4$, $YbZnCu_4$ $n_e <$ 1e/atom Slow crossover

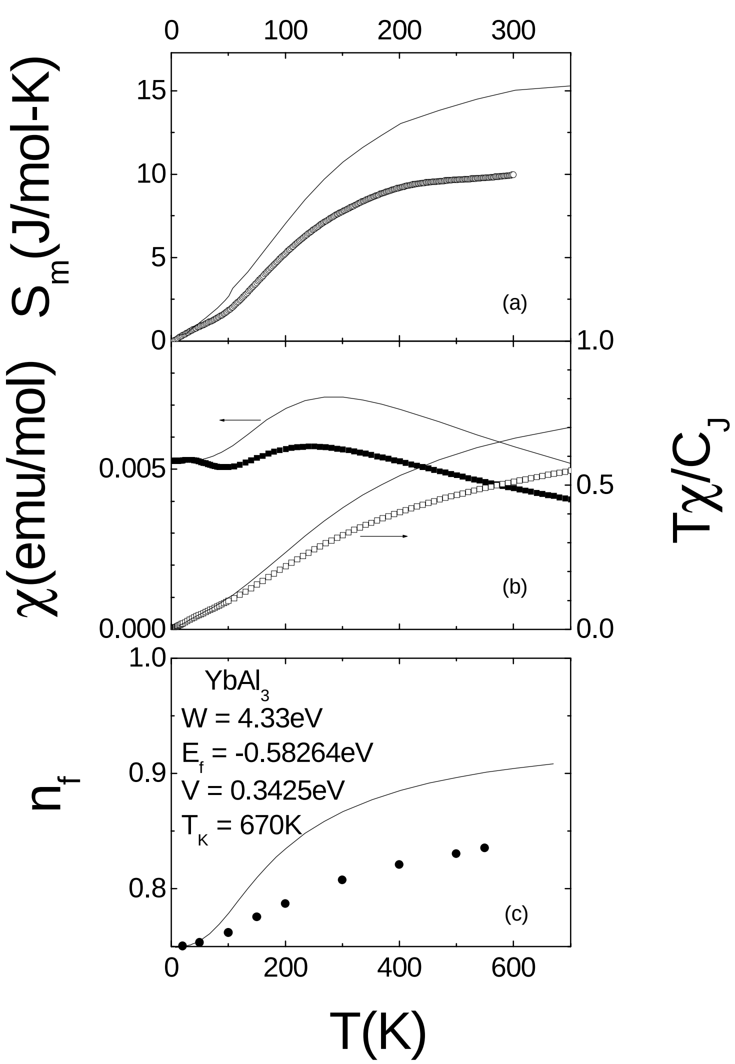

For $YbAl_3$
$n_e = 1/R_He = 0.5$ e/atom

slow crossover is observed for entropy, susceptibility and 4f occupation number

Symbols: expt. Data
Lines: AIM

Cornelius et al
PRL88 (2002) 117201

Low temperature form factor and susceptibility anomalies in $CePd_3$

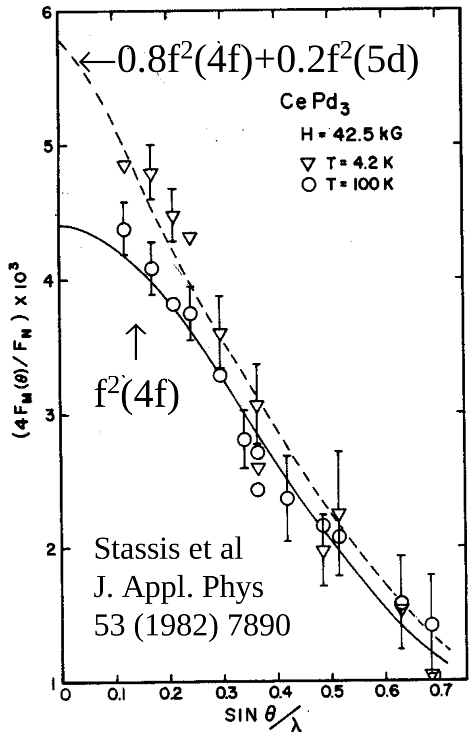

The neutron form factor measures the spatial distribution of magnetization around the Ce or Yb site.

At high T the form factor has the same Q (or r) dependence $f^2(4f;Q)$ as the 4f radial function. (Solid line)

In $CePd_3$ at low T a more diffuse 5d component $f^2(5d;Q)$ is present:

$$f^2(Q) = a^2\, f^2(4f) + (1-a^2)\, f^2(5d)$$

(Dashed line)

Thompson et al, J. Appl. Phys. 53 (1982) 7893

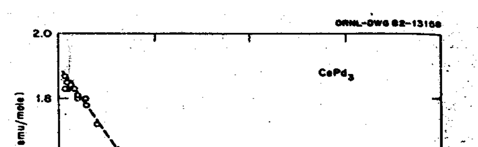

Figure 1. The magnetic susceptibility χ per formula unit of CePd3 versus temperature T. (Note that the vertical scale has been expanded).

The 5d contribution gives rise to an anomalous increase in the low temperature (T < 50K) susceptibility over and beyond the Kondo peak (which is near 150K).

Low temperature anomalies in $YbAl_3$

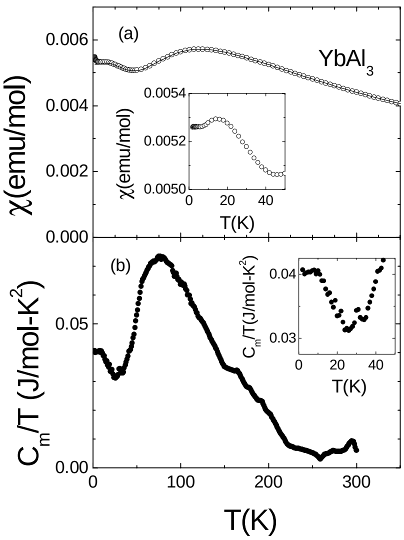

Cornelius et al
PRL 88 (2002) 117201

Above 40K the **susceptibility** and **specific heat** correspond qualitatively to the predictions of the AIM.
Below 40K, **anomalies** are observed. These anomalies are destroyed rapidly by alloying (Bauer et al) indicating the importance of lattice coherence in the anomalies.
The anomalies occur on the same temperature scale T_{coh} as the fully renormalized optical conductivity and the Fermi liquid T^2 resistivity.
We note $T_{coh} \sim n_f T_K / (2J+1)$

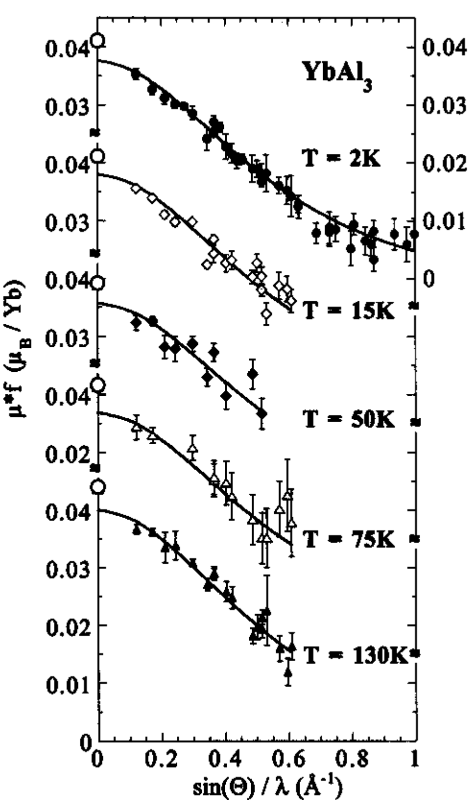

Hiess et al
J Phys: Cond. Mat 12 (2000) 829

However, in $YbAl_3$, there is ***no form factor anomaly*** -- the magnetization density is that of the 4f orbital at all temperatures (solid lines).

New peak in low temperature spin dynamics

We have seen that for most temperatures and energies the magnetic neutron scattering in $YbAl_3$ follows the predictions of the AIM, with a Lorentzian power spectrum with E_0 = 40meV and Γ = 25meV

Mrani, PRB 50 (1994) 9882

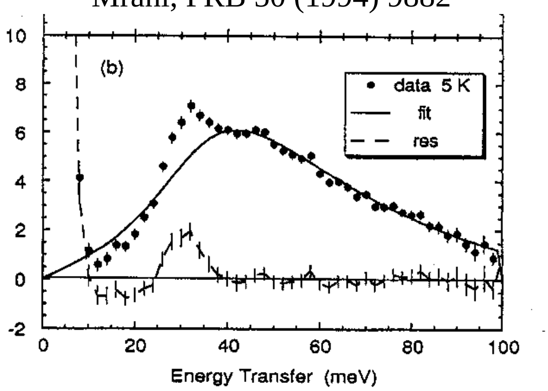

At low T, there is an additional narrow peak with
E_0 = 30meV and Γ = 5meV
This peak vanishes above 50K, and hence appears to be a property of the fully coherent ground state.

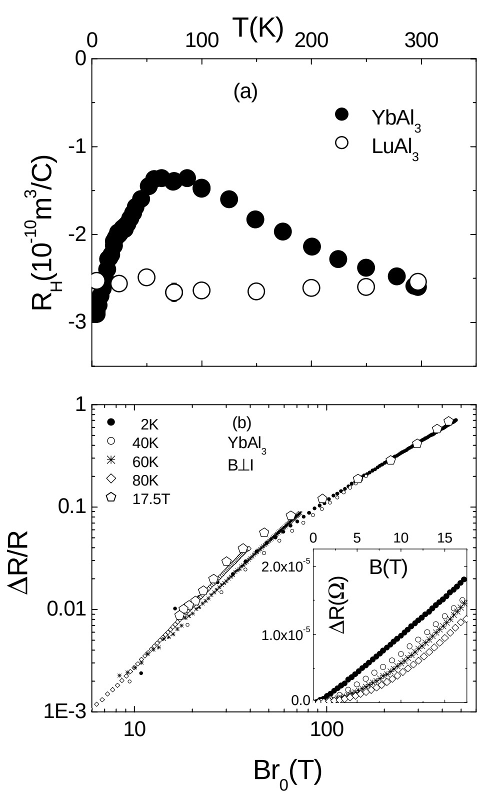

Magnetotransport anomalies

Anomalies in the Hall coefficient and magnetoresistance are observed in this same temperature range.

Since $R_H \sim 1/ne$ this suggests a change in carrier density. The onset of coherent Fermi liquid behavior appears to involve a change in the Fermi surface.

Cornelius et al
PRL 88 (2002) 117201

Field dependent masses in $YbAl_3$

Ebihara, Cornelius, Lawrence, Uji and Harrison

cond-mat/0209303

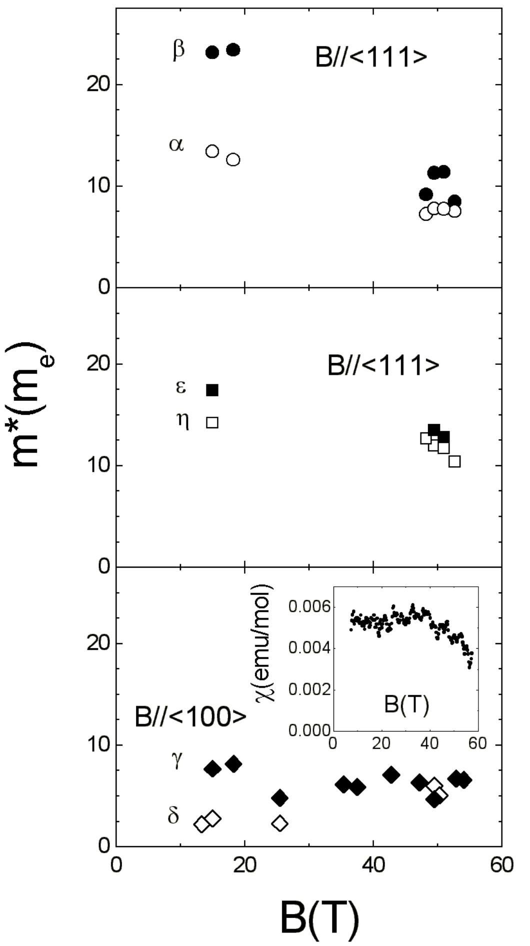

High field dHvA shows that the effective masses for H//<111> decrease substantially for H > 40T. This field is much smaller than the Kondo field $B_K = kT_K/gJ\mu_B$ required to polarize the f electrons, but is of order k_BT_{coh}/μ_B.

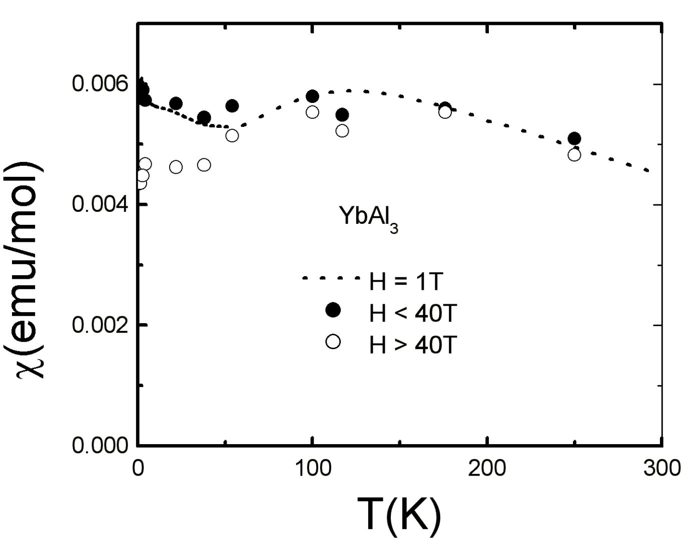

A field of this magnitude also suppresses the low temperature susceptibility anomaly.

It is as though that the system exhibits a crossover from a anomalous high mass Fermi Liquid state to a non-anomalous moderately enhanced Fermi liquid state for $\mu_BH > k_BT_{coh}$.

EFFECT OF DISORDER ON THE LOW TEMPERATURE ANOMALIES

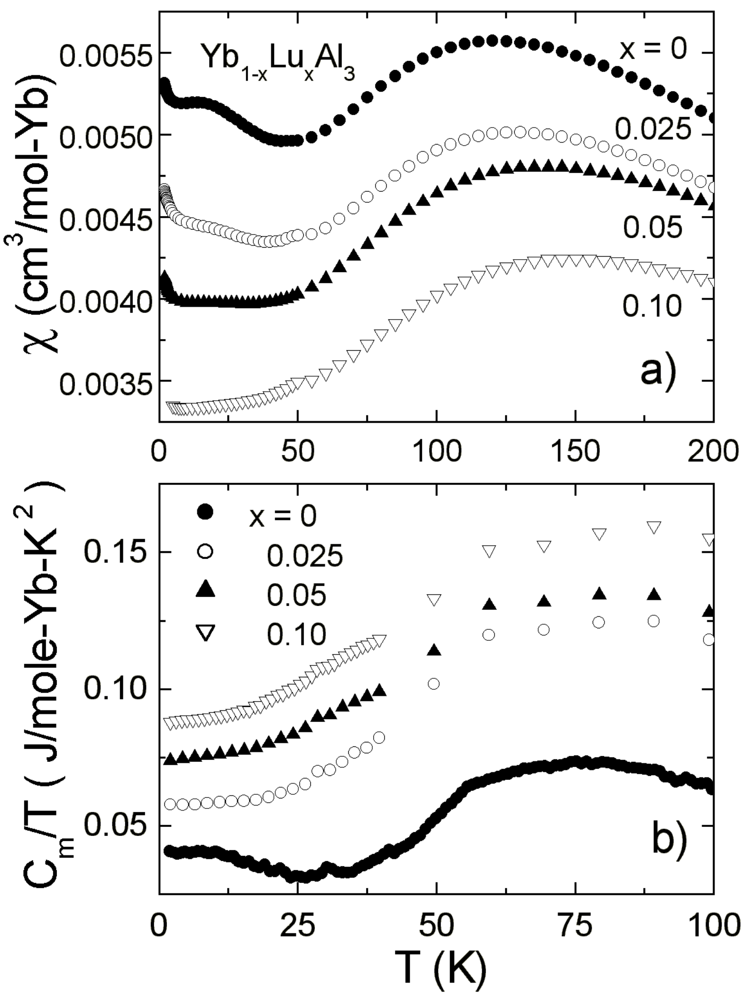

The low temperature anomalies in the susceptibility and specific heat are very sensitive to alloy disorder, and disappear for alloy concentrations as small as x = 0.05 in $Yb_{1-x}Lu_xAl_3$. Apparently the enhanced masses observed below T_{coh} are very sensitive to lattice coherence.

Summary

The Kondo temperature T_K ~ 500K sets the main scale for the crossover from local moment behavior to nonmagnetic behavior in IV compounds. At high T the behavior is that of uncorrelated Kondo impurities; the AIM works qualitatively (sometimes quantitatively) for χ (T), n_f(T) and $\chi''(\omega)$. Below a lower temperature scale for the onset of coherence (T_{coh} ~ 30-50K)

The following should occur in all compounds:

1) The resistivity shows T^2 behavior. — All compounds

2) Onset of fully renormalized mass in the optical conductivity — Direct observation: $CePd_3$; Extrapolation: $YbAl_3$; $YbFe_4Sb_{12}$

3) Onset of fully developed hybridization gap — $CePd_3$; $YbFe_4Sb_{12}$; $YbAl_3$

4) Large effective masses in dHvA — $CeSn_3$, CeNi, $YbAl_3$

5) Anomaly in the Hall coefficient indicating a change in carrier density. — $CeBe_{13}$, $CePd_3$, $CeSn_3$, $YbAl_3$

6) FL scattering and Q-dependent gap scattering expected in $\chi''(Q,\omega)$ — Not observed for any compound

The following anomalies occur in some, but not all, compounds:

7) New peak in χ — $CePd_3$, $YbAl_3$ (*Maybe* $CeSn_3$, *not* $YbAgCu_4$)

8) New peak in C/T — $YbAl_3$

9) New peak in the spin dynamics: — $YbAl_3$, (*Maybe* CeNi; *not* $YbAgCu_4$)

10) 5d contribution to the form factor — $CePd_3$ (*Maybe* $CeSn_3$, *not* $YbAl_3$)

11) Suppression of dHvA mass at $B \sim k_B T_{coh}/\mu_B \ll B_K = k_B T_K / gJ\mu_B$ — $YbAl_3$

12) Slow crossover from low temperature Fermi liquid to high temperature paramagnet — $YbAl_3$, $YbMgCu_4$ (*not* $YbAgCu_4$, $YbTlCu_4$)